

Salt-water intrusion processes in groundwater; novel computer simulations, field studies and interception techniques

H.-J. DIERSCH

Joint Application Research Group in Hydrogeology and Geothermic, Academy of Sciences of the GDR, Institute for Mechanics Karl-Marx-Stadt, DDR-9010, German Democratic Republic

P. NILLERT

Joint Application Research Group in Hydrogeology and Geothermic, VEB Geothermie Neubrandenburg, German Democratic Republic

Abstract Current model applications and field-related studies focusing on salt-water upconing below pumping wells are presented. The paper gives attention to a new interception technique termed salt-water-preventive well (SPW). Its effectiveness and usefulness have been proved in field tests and benchmarked with model predictions. For transient nonlinear salt-water intrusion problems, a one-step Newton predictor-correction finite element scheme is applied.

INTRODUCTION

The utilization and management of aquifers influenced or partially saturated by saline water cause many serious problems encountered in current research and practice. In the past, much work has been undertaken by field studies, experimental and theoretical investigations to understand and to describe the behaviour of salt-water intrusion processes in subsurface water resource systems (Reilly & Goodman, 1985). Beside the progress made, there is now as ever a series of open questions in understanding salt-water dynamics and the practice necessitates better modelling and field-related observations.

A numerical study of the salt-water upconing mechanism below pumping wells (Diersch *et al.*, 1984) brought to light a proper transient intrusion development termed as overshooting effects. The predictions have been verified and discussed on an analytical basis (Thiele & Diersch, 1986). As studied previously (Diersch & Nillert, 1984) sharp-interface fresh-water/salt-water approaches can be totally unsuitable if there are interests in moderately saline processes and in salinity of the pumped water. Recently, it has been found (Nillert *et al.*, 1988) that numerical simulations based on a general transport model are in good agreement with long-term field observations of salt-water upconing and well intrusion. On the other hand, engineers and policy makers have been increasingly faced with prediction of salt-water interception and remedial techniques. Numerical simulation can clear the dynamics of such complex processes to value the design variables (e.g. location of well screens, pumping and injection rates) for an effective and

efficient interception operation. As a new interception technique, so-called salt-water-preventive wells (SPW) have been proposed.

The purpose of the present paper is twofold:

- (a) to highlight current model application and field-related studies focussing on salt-water upconing below pumping wells and the SPW interception technique, and
- (b) to discuss aspects in mathematical modelling of salt-water/fresh-water systems based on general transport models.

For the finite element method, an alternative solution strategy regarding transient nonlinear salt-water intrusion problems based on a one-step Newton predictor-corrector technique is used to govern the solution of the coupled flow and transport process.

MATHEMATICAL MODEL

The density-coupled salt-water transport in groundwater is represented by the following set of partial differential equations:

$$\frac{\partial q_i}{\partial x_i} = 0 \quad (1)$$

$$q_i = \phi v_i = -K_{ij} \left[\frac{\partial h}{\partial x_j} + \frac{\rho - \rho_0}{\rho_0} \delta_{kj} \right] \quad (2)$$

$$\phi \frac{\partial C}{\partial t} + \frac{\partial}{\partial x_i} (q_i C) - \frac{\partial}{\partial x_i} \left[\phi D_{ij} \frac{\partial C}{\partial x_j} \right] = \phi Q_c \quad (3)$$

with

$$\rho = \rho_0 \left[1 + \chi \frac{C}{C_s} \right] \quad (4)$$

$$D_{ij} = (D_0 + \beta_T V) \delta_{ij} + (\beta_L - \beta_T) \frac{v_i v_j}{V} \quad (5)$$

where

- q_i = Darcy flux,
- ϕ = porosity,
- v_i = pore velocity,
- K_{ij} = hydraulic conductivity,
- h = hydraulic head,
- ρ, ρ_0 = density of salt-water and fresh-water, respectively,
- C = salinity,
- D_{ij} = hydrodynamic dispersion,
- Q_c = sink/source,
- χ = density difference ratio,
- C_s = maximum salinity,

- D_o = diffusion,
 β_L, β_T = longitudinal and transverse dispersivity, respectively,
 V = absolute pore velocity,
 δ_{ij} = Kronecker tensor,
 x_i = Cartesian axis,
 k = gravity direction.

The spatial discretization by finite elements requires the matrix system to be solved for h , q_i and C :

$$\begin{aligned}
 Sh &= F(C) \\
 Aq &= B(h, C) \\
 PC + D(q, C)C &= R
 \end{aligned}
 \tag{6}$$

where the main functional dependence is shown in parenthesis. The transient matrix system (6) is highly coupled for strong density effects. The solution algorithm preferred is embedded in a predictor-corrector procedure. A thorough description of the solution algorithm is given in Diersch (1988). Avoiding further mathematical details we designate only some remarkable features:

For the salinity C predictor formulae are used to govern the nonlinear terms. The corrector solutions for salinity involve a one-step Newton scheme. The history vectors C for the salinity are determined. Having the approximation error for salinity

$$\mathfrak{e}^{n+1} = \frac{1}{2}(C^{n+1} - C_p^{n+1})
 \tag{7}$$

where superscript n denotes the time point, and C and C_p correspond to the corrector and predictor solutions, respectively, the tactic of time step control is then as follows:

Keeping the error within each time step below a pre-set level $\epsilon \sim 10^{-3}$, defined as

$$\epsilon = \frac{\|\mathfrak{e}^{n+1}\|}{\|C^{n+1}\|}
 \tag{8}$$

where $\|\cdot\|$ corresponds to the Euclidean norms, the acceptable size for the next time step can be computed from

$$\Delta t_{n+1} = \Delta t_n \left[\frac{\epsilon \|C^{n+1}\|}{\|\mathfrak{e}^{n+1}\|} \right]^{1/(\sigma+1)}
 \tag{9}$$

where $\sigma \in (1,2)$ according to the order of predictor-corrector scheme used.

The tactic of approximating error control via the time step size selection subjected to expression (9) contains following three criteria:

- (a) if $\Delta t_{n+1} \geq \Delta t_n$, the solution is accurate within the bound pre-assigned by ϵ ;
- (b) if the condition $\|\delta^{n+2}\| < \phi \in \|\mathcal{C}^{n+1}\|$ (with $\phi \sim 1.5$) is violated, the error is deemed unacceptably large and the solution at time point $n + 1$ must be rejected and the step has to be repeated with a reduced time increment;
- (c) if $\phi^{-1/(1+\sigma)} \Delta t_n \leq \Delta t_{n+1} < \Delta t_n$, the solution at $n + 1$ is accepted, however, the change of the time step Δt_{n+1} is ignored.

The above algorithm monitors the solution process via the local time error estimation in which the size of the time step is cheaply and automatically varied in accordance with temporal accuracy requirements. In many practical tasks it has been proved to be a well-behaved and robust procedure which has numerical advantages over common iterative methods.

The procedures outlined have been incorporated in the user-oriented computer code FEFLOW (Diersch & Israel, 1986). The code guarantees a high portability and is equipped with facilities of today's finite element standard (mesh generator, RCM nodal ordering, resolution control, active column equation solvers, etc.).

SALT-WATER UPCONING

The investigations refer to a long-term field experiment of a test well in a layered aquifer which is underlain by salt water with a maximum salinity of about 4600 mg l^{-1} . The schematic cross section and geological profile of the aquifer are shown in Fig. 1. The test well was installed with a series of samplers placed at different elevations to observe the transient rise of the saltwater upconing. The representative meridional computational domain and its finite element idealization are depicted in Fig. 2. Table 1 shows the hydraulic and salinity parameters used in the flow and transport equations. The aquifer with a thickness of 19 m consists of four layers with different hydraulic conductivities as given in Table 1.

In Fig. 3, the simulation results as salinity breakthrough curves over the study period reaching from April 1985 to February 1986 are compared with the observations of four samplers (OP, MP i , $i = 1, 3$). For the upper and lower samplers quite good agreement has been found, while differences for the MP1 values occur. The retarded behaviour of the observations is likely due to the radial flow system approach in the model whereas the natural system reveals more three-dimensional effects.

A nearly steady-state salt-water upconing has been established after about seven months. At the end of October 1985 the well abstraction was increased from 50 to $75 \text{ m}^3 \text{ h}^{-1}$. Accordingly, it was interesting to note that no response of salinities to this hydrodynamic action occurred which sharply contradicts the idea based on interface concepts where the salt-water upconing rise should be a strong function of well abstraction. As presented in Thiele & Diersch (1986), the salt-water intrusion process is independent of the absolute

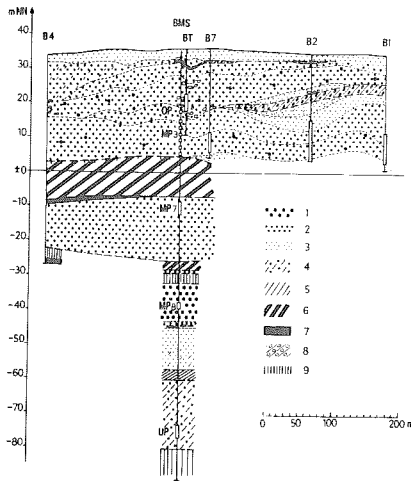


Fig. 1 Schematic cross section and geologic profile of test aquifer for salt-water upconing.

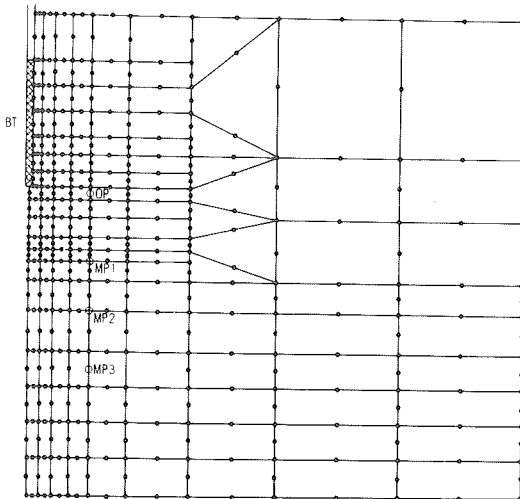


Fig. 2 Meridional computational domain, finite element mesh used, locations of well screen (BT) and samplers (OP, MP1, MP2, MP3).

value of velocity; however, for layered aquifers it depends on the ratio of hydraulic conductivities (lower layer to upper one)

$$\omega = \frac{K_{\text{lower}}}{K_{\text{upper}}} \quad (10)$$

Table 1 Hydraulic and transport parameters used

Saturated thickness	19 m
Well abstraction	50 m ³ h ⁻¹ (t ≤ October 1985) 75 m ³ h ⁻¹ (t > October 1985)
Hydraulic conductivity	
upper layer 1 (5.50 m)	6 × 10 ⁻⁴ m s ⁻¹
layer 2 (5.00 m)	2.2 × 10 ⁻⁴ m s ⁻¹
layer 3 (2.75 m)	1.8 × 10 ⁻⁴ m s ⁻¹
lower layer 4 (5.75 m)	1.4 × 10 ⁻⁴ m s ⁻¹
Longitudinal dispersivity	0.75 m
Transverse dispersivity	0.0375 m
Porosity	0.3
Diffusion coefficient	10 ⁻⁹ m ² s ⁻¹
Maximum salinity	4600 mg l ⁻¹
Background salinity	70 mg l ⁻¹

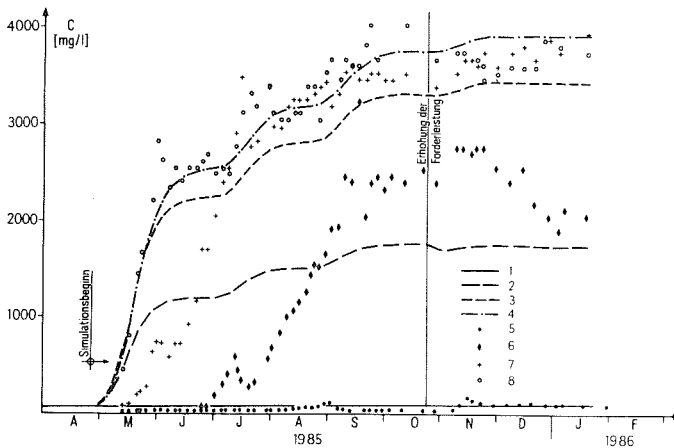


Fig. 3 History of observed (dotted) and computed (lined) salinities in four samplers (OP, MP1, MP2, MP3).

The salinity must then be a function according to

$$C \sim \frac{\omega \beta C_s + (1 - \beta) C_o}{\omega + (1 - \beta)} \tag{11}$$

where C_s and C_o are the maximum and background salinities, respectively, and β is the geometric ratio of thickness of salt-water zone to the entire aquifer thickness which was assumed as 1.5 m/19 m. For more discussion see Nillert *et al.* (1988).

As an important characteristic parameter for the SPW operation, the injection ratio α is defined as

$$\alpha = \frac{Q_{IB}}{Q_{IB} + Q_{PB}^{net}} \quad (13)$$

in the range $0 \leq \alpha < \frac{1}{2}$. In a series of numerical experiments, the efficiency of the SPW has been recognized depending on the α parameter, the hydrogeologic and hydraulic conditions, the elevations of injecting and pumping screens and other parameters. Based on these investigations a SPW has been designed and optimized for our test aquifer mentioned above. As the salt-water upconing has fully been established (period after February 1986), the test well was converted into a SPW operation. Figure 5 exhibits the observed and simulated well salinity transients are different α values when the SPW came into operation. In Fig. 6 (a) and (b), the measured and simulated vertical salinity distributions dependent on the α -ratio show how the SPW works.

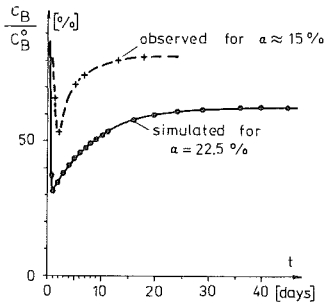


Fig. 5 Observed and simulated development of well salinity for SPW operation (C_B = transient well salinity, C_B^0 = initial well salinity, i.e. without SPW).

The effectiveness of the SPW for the test aquifer is shown in Fig. 7 showing the reduction of salinity in pumped water related to the initial state (i.e. without SPW measure) vs. the injection ratio α . A quite good agreement between observations and finite element results has been found. For the test well, a salt-water contaminant reduction in the pumped water to 60% for $\alpha = 27\%$ has been reached in our test series. Under the constraints that the net production of the well is unchanged, the SPW is devised to bypass and remove extracting water for re-injection and the SPW must work under super-critical salt-water upconing conditions (Diersch & Nillert, 1984). It has proved the SPW to be an efficient interception alternative where the unavoidable rise of salt-water upconing (if the abstraction is sufficiently high) can be carefully stabilized

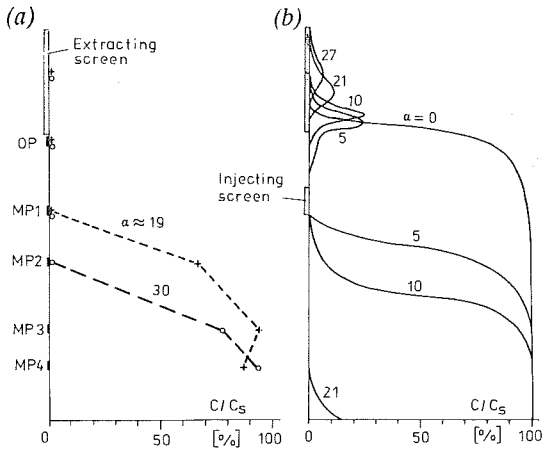


Fig. 6 Vertical salinity distribution for the SPW test vs. the α -ratio (in percent): (a) measured results (along sampler line 2.6 m far from well axis); (b) simulated results (along the well axis).

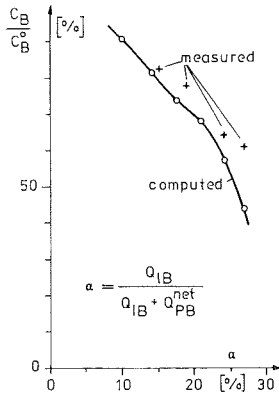


Fig. 7 Measured and simulated salinities of pumped water vs. the injection ratio α .

on the lowest level possible and the salt-water content in the pumped water is reduced to acceptable levels in practice. Depending on the particular geohydrologic conditions and realizable hydraulic measures, a salinity reduction below 50% for reasonable injection rates is predicted. Further studies and field experiments are currently underway.

COMPUTATIONAL ISSUES AND CONCLUSIONS

Simulation models are powerful tools to control salt-water intrusion and to devise appropriate interception and remedial strategies. A predictor-corrector finite element procedure is used to circumvent previous mathematical difficulties and to support user-friendly solution for general salt-water intrusion processes. In Fig. 8 is presented a typical time step history obtained for a salt-water-driven intrusion process from a deposit (Diersch, 1988). This information actually gives significant insight into the "physics" of the intrusion process and the numerical effort necessary.

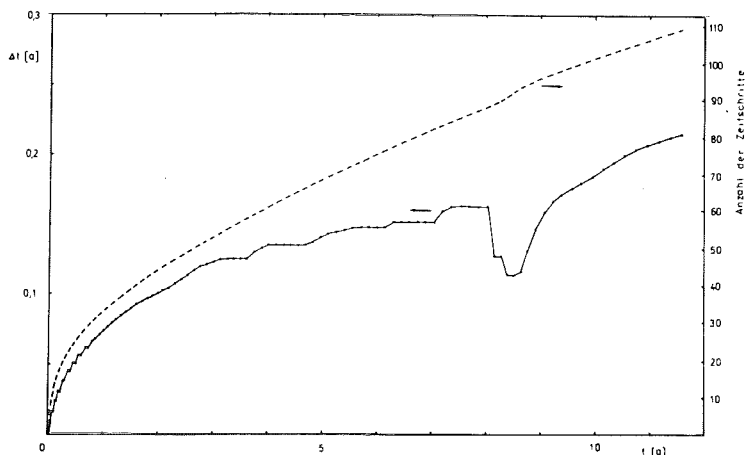


Fig. 8 Time step history and number of time steps.

In the further development and application, optimization models for interception/remedial strategies running on interactive graphic modelling systems are becoming of increasing importance. A prototype model version is presented by Fedra & Diersch (1989).

Acknowledgements We are grateful to M. Günther for its support in the field study and perseverance regarding our SPW project.

REFERENCES

- Diersch, H.-J., Prochnow, D. & Thiele, M. (1984) Finite-element analysis of dispersion-affected saltwater upconing below a pumping well. *Appl. Math. Modelling* 8 (10), 305-312.
- Diersch, H.-J. & Nillert, P. (1984) Untersuchung zur Dynamik geogen bedingter Salzkontaminationen an Vertikalfilterbrunnen. *Z. Angew. Geol.* 30 (2), 93-104.
- Diersch, H.-J. & Israel, Ch. (1986) Finite element simulator FEFLOW - computer program to solve areal groundwater flow and mass/heat transport: Part 1 Horizontal mass transport code. Part 2 Vertical mass transport code. Part 3 2-D heat transport code.

- User's Manual*. Institute for Mechanics of the Academy of Sciences of GDR, Karl-Marx-Stadt.
- Diersch, H.-J. (1988) Finite element modelling of recirculating density-driven saltwater intrusion processes in groundwater. *Adv. Wat. Resour.* 11 (1), 25-43.
- Fedra, K. & Diersch, H.-J. (1989) Interactive groundwater modelling: colour graphics, ICAD and AI. In: *Groundwater Management: Quantity and Quality* (Proc. Benidorm Symp., October 1989), 305-320. IAHS Publ. no. 188.
- Huisman, L. & Olsthoorn, T. N. (1983) *Artificial Groundwater Recharge* - Section 9: Intrusion Control, 275-286. Pitman Advanced Publishing Program, Boston, USA.
- Nillert, P., Diersch, H.-J., Günther, M. & Lehmann, H.-W. (1988) Feldtest zum Salzwasser-aufstieg unter Brunnen. *Z. Angew. Geol* 34 (6), 161-169.
- Reilly, T. E. & Goodman, A. S. (1985) Quantitative analysis of saltwater-freshwater relationships in groundwater systems - a historical perspective. *J. Hydrol* 80 (1/2), 125-160.
- Thiele, M. & Diersch, H.-J. (1986) "Overshooting" effects due to hydro-dispersive mixing of saltwater layers in aquifers. *Adv. Wat. Resour.* 9 (1), 24-33.